Version: July 1, 2022

Nucleus of the lateral olfactory tract (NLOT): a hub linking water homeostasis-associated SON-AVP circuit and neocortical regions to promote social behavior under osmotic challenge

Oscar R. Hernández-Pérez[1,3], Vito S. Hernández[1,3], Mario A. Zetter[1], Lee E. Eiden[2], and Limei Zhang[1c]

[1] Department of Physiology, School of Medicine, National Autonomous University of Mexico, Mexico
[2]National Institute of Mental Health, National Institute of Health, Bethesda, MD, USA
[3]Authors contributed equally to this work
[c] Corresponding author: Limei Zhang MD, PhD, limei@unam.mx

Abstract

Homeostatic challenges increase the drive for social interaction. The neural activity that prompts this motivation remains poorly understood. Here, we identify direct projections from hypothalamic supraoptic nucleus (SON) to the cortico-amygdalar nucleus of the lateral olfactory tract (NLOT). Dual in situ hybridization (DISH) with probes for PACAP, and VGLUT1, VGLUT2, V1a and V1b revealed a population of vasopressin-receptive PACAPergic neurons in NLOT layer 2 (NLOT2). Water deprivation (48 hours, WD48) increased sociability compared to euhydrated subjects, assessed with the three-chamber social interaction test (3CST). Fos expression immunohistochemistry showed NLOT and its main efferent regions had further increases in rats subjected to WD48+3CST. These regions strongly expressed PAC1 mRNA. Microinjections of AVP into NLOT produced similar changes in sociability to water deprivation, and these were reduced by co-injection of V1a or V1b antagonists along with AVP. We conclude that during challenge to water homeostasis, there is a recruitment of a glutamatergic-multi-peptidergic cooperative circuit that promotes social behavior.

Keywords: V1a, V1b, PAC1, VGLUT1, agranular insular cortex, claustrum, fluorogold, dual ISH

Supported by grants: UNAM-DGAPA-PAPIIT- PAPIIT-IN216918 & GI200121 & CONACYT-CB-283279 (LZ); MH002386, NIMH, NIH, USA (LEE).

1. INTRODUCTION

Neuropeptides acting as neurotransmitters in the brain participate in circuits which monitor multiple environmental inputs, and access brain state-related information, in order to produce highly integrated responses that are appropriately tuned to the specifics of a given situation requiring motor decision-making (action) [1]. An area of research relevant to the general question of how multiple-circuit integration leading to specific behaviors occurs, is the study of the microanatomy, neurochemistry, and cellular and behavioral functions of vasopressinergic magnocellular neurosecretory neurons (AVPMNNs) of the mammalian brain. This is because AVPMNNs have very well-defined roles as neurosecretory neurons that release vasopressin into the bloodstream for hormonally-driven osmotic regulation (hydromineral *homeostasis*), and as well, via dual projections within the brain parenchima, release vasopressin as a neurotransmitter to affect limbic, hypothalamic, and other brain circuits that participate in behavioral prioritization responsive to competing homeostatic drives, i.e. *allostasis* [2].

In previous studies, we have demonstrated that activation of the AVPMNN system in the hypothalamic paraventricular nucleus (PVN) by alteration of osmotic balance through water deprivation or salt loading activates both limbs of this dually-projecting system. This results not only in changes in blood levels of vasopressin indicative of hormonal homeostatic regulation, but changes in electrical activity and even synaptic protein expression at vasopressinergic terminal field regions of hippocampus, amygdala, locus coeruleus and other locations. These are indicative of potentially profound effects on behaviors[3-9] and thus linking the original homeostatic osmoregulatory drive, to allostatic drives that must act in concert with it.

Social behavior is one of the core factors facilitating an individual's chances of survival. However, the neural substrates underlying this behavioral are only now being uncovered. Vasopressin has been shown to participate in several aspects of social behavior. For instance, mice deficient for V1a and V1b receptors show social deficits[10-12]; Brattleboro rats lacking AVP expression have reduced social interaction [13, 14]**;** and altered AVP transmission has been described in pathologies characterized by social deficits [15, 16].

In contrast to the PVN, the hypothalamic supraoptic nucleus (SON), which contains another major population of AVPMNNs responsible for controlling body water balance, has been less investigated regarding ascending projections, as well as concerning its roles in behavioral adaptation. This lack of information is mainly due to its deep location at the base of the brain. Using in vivo electrophysiological recording, Inyushkin et al [17] demonstrated a

clear dual projection system, neurohypophysial and central, from SON AVPMNNs, and suggested the existence of projections from these neurons in the SON that are much more widespread and longer than had previously been suspected. SON's innervation to dorsal and ventral hippocampus and central amygdala was subsequently demonstrated using the fluorogold method [6, 18].

The nucleus of the lateral olfactory tract (NLOT) is located in the anterior cortico-amygdalar region adjacent to the ventral surface of the brain. This structure is connected with the main olfactory bulb, and the piriform and insular cortices, and is implicated in feeding behavior [19]. It has been described as a three-layered structure[20]. Its heterogeneous neuronal composition suggests different neuroepithelial origins of the cells that populate its three layers [21].

The aim of the present study was to evaluate whether or not NLOT is a brain region is a brain region containing vasopressin-responsive neurons important in mediating the social effects of AVP. By analyzing Golgi-Cox staining, we observed direct projections from SON to the nucleus of lateral olfactory tract (NLOT) of cortico-amygdalar complex. Fluoro-Gold injection into the NLOT revealed retrogradely labelled AVP-positive somata in SON. We previously reported that the main neuronal population of NLOT co-expresses the neuropeptide PACAP and vesicular glutamate transporters 1 and 2 (VGLUT1 and VGLUT2). Here, using the dual in situ hybridization method we demonstrate that the principal population of PACAP/VGLUT1/VGLUT2 neurons co-expresses vasopressin receptors V1a and V1b. Considering these observations, we devised a behavioral experiment using 48 hour water deprivation (WD48) and a three-chamber social interaction test (3CST) [22, 23], designed to quantify the level of sociability, defined as the tendency to approach and remain proximal to an unfamiliar conspecific (we called "rat *stranger*" hereafter). WD48 significantly increased the social behavior. Fos expression assessment showed AVP-MNNs and PACAP-NLOT regions and their efferents had further increases in rats subjected to WD48+3CSI. The efferent regions of PACAP-NLOT strongly expressed PAC1 mRNA. AVP and NLOT involvement in this increased sociability and Fos expression was further demonstrated through microinjections of AVP, AVP+V1a or V1b antagonists, targeting NLOT, that AVP microinjection alone produced similar increase produced by WD24 but if applied together with V1a or V1b antagonists, the AVP-stimulated increases were ablated. These results suggest that under situations where homeostasis is compromised by osmotic challenge, there is a recruitment of a glutamatergic-multi-peptidergic cooperative circuit that is able to promote behavioral adaptation through social interaction.

2. EXPERIMENTAL PROCEDURES

112 2.1 Animals
113
114 One hundred and forty-four adult male Wistar rats of 280 ± 20 g were obtained from the
115 local animal facility. Rats were housed four per cage in a controlled environment
116 (temperature 24 ºC and illumination 12 h/12 h (lights on at 7:00 to 19:00 h) with water and
117 food *ad libitum*). All animal procedures were approved by the *Comision de Investigacion y*
118 *Etica de la Facultad de Medicina, Universidad Nacional Autonoma de Mexico* (approval
119 number: CIEFM-062-2016). Efforts were taken to minimize animal suffering throughout all
120 experimental procedures.
121
122 2.2 Social behavior assessment under water deprivation
123
124 A first experiment was devised to assess the effects of water deprivation on social behavior.
125 Twenty-four rats were randomly assigned to 48h of water deprivation (WD48, n=14) or water
126 *ad libitum* (control, n=12). The rationale for this manipulation was that WD48 up-regulates
127 the metabolic activity of the hypothalamic AVPMNNs with only a modest increase in plasma
128 osmolarity [5, 24]. Social behavior was tested in the three-chamber social interaction test
129 (3CST). The test was carried out essentially as described elsewhere [22, 23]. Briefly, testing was
130 conducted in a three-chambered box made of acrylic (100 cm x 30 cm x 30 cm), the central
131 chamber (20 cm x 30 cm) and two distal chambers (40 cm x 30 cm) each. Chambers were
132 connected via open doors (10 cm x 10 cm). One day before the experiment, the rats were
133 allowed to explore the apparatus freely for 10 min to be habituated to the experimental
134 device. On the day of the experiment, an empty cage was placed in a compartment (*non-*
135 *social* compartment), a similar cage containing a male rat *stranger* was placed in the opposite
136 chamber (*social* compartment). The experiment started by putting the experimental subjects
137 in the central chamber of the apparatus and allowed access to all chambers for 10 minutes.
138 The time the rat spent in the *social* chamber and the number of approaches/sniffing to the
139 rat *stranger* were scored.
140
141 2.3 Immunohistochemistry and immunofluorescence
142
143 Rats were deeply anesthetized with sodium pentobarbital (63 mg/kg, Sedalpharma, México)
144 and perfused transaortically with 0.9% NaCl followed by cold fixative containing 4%
145 paraformaldehyde in 0.1 M sodium phosphate buffer (PB, pH 7.4) plus 15% v/v saturated
146 picric acid solution for 15 min. Brains were immediately removed, blocked, thoroughly rinsed
147 with PB 0.1M, and sectioned at 70 µm from forebrain to hindbrain using a Leica VT 1000S
148 vibratome. Sections were blocked with 20% normal donkey serum in Tris-buffered (0.05 M,
149 pH 7.4), NaCl (0.9%), plus 0.3% of Triton X-100 (TBST) for 1h at room temperature,
150 immunoreacted overnight with rabbit anti-Fos primary antibody (SC-52, 1:1000, Santa Cruz

151 Biotechnology, Santa Cruz, CA, USA) or rabbit anti vasopressin primary antibody (kind gift
152 from Professor Ruud Buijs), washed and incubated with secondary biotinylated antibody
153 (goat anti-rabbit, vector BA1000) followed by incubation in Vectastain Elite ABC kit solution
154 (Vector Labs, Burlingame, CA, USA) and detection with a DAB-peroxidase reaction. For
155 Immunofluorescent processing we used a secondary donkey anti rabbit Alexa 594
156 fluorescent antibody. Some photomicrographs were presented digitally inverted (negative
157 mode) to enhance the visibility of DAB labelled AVP fibers.
158
159 2.4 Neuronal Activation assessment after 3CST
160
161 To assess the pattern of neuronal activation induced in the brain by the 3CST and/or water
162 deprivation, we formed four groups of n=5 rats: Control (same conditions as other groups
163 but undisturbed until perfusion time); Social interaction (rats that were under ad-libitum
164 water access until the 3CST); 48h WD (rats deprived of water during the 48h previous to the
165 perfusion with no other disturbance) and 48h WD + social Interaction (rats that underwent
166 48h of water deprivation before the 3CST experiment). Rats evaluated by the 3CST were
167 perfused 60 min after finishing the behavioral test; the other groups were perfused at the
168 same circadian time. After perfusion, immunohistochemistry against Fos was performed as
169 described above.
170
171 Regions of interest were identified using a low magnification objective with
172 referencing to a standard rat brain stereotaxic atlas [25]. The average number of Fos+ nuclei
173 in each identified region was quantified under a 40x objective (0.196 mm^2). Two comparable
174 fields per area in each rat were quantified by two independent researchers. A table
175 comparing the four groups was constructed with semi-quantitative criteria. i.e., "+": 1 to 25
176 per field; "++": 26 to 50 per field; "+++": 51 to 75 per field; "++++": 76 to 100 per field;
177 "+++++": >100 per field (field area: 0.196 mm2, for simplicity we used 0.2 mm^2).
178
179 2.5 Fluorogold retrograde tracing
180
181 The Fluorogold retrograde method was performed as previously reported [6, 18]. Rats (male,
182 n=4, 280-300g) were deeply anaesthetized using a 1:1 mixture of xylazine (20 mg/ml, Procin,
183 Mexico) and ketamine (100 mg/ml, Inoketam, Virbac, Mexico) administered as a dose of 1
184 ml/kg body weight intraperitoneally. Rats were fixed in a stereotaxic frame, and the
185 retrograde tracer Fluoro-Gold (FG, Fluorochrome, LLC, Denver, Colorado 80218, USA),
186 dissolved to a concentration of 1% in 0.1 M cacodylate buffer (pH 7.5), was delivered into
187 the nucleus of the lateral olfactory tract (NLOT) using a glass micropipette with an inner tip
188 diameter of around 40 µm. Current used for iontophoresis was of 0.1 µA with a 5-s pulse-

189 duration and a 50% duty cycle during 20 min. The coordinates for positioning the pipette in
190 NLOT were: AP -1.4 mm, ML ± 3.2 mm from bregma, and DV -9.4 mm from the skull surface,
191 according to a stereotaxic atlas [25]. Additional time-lapse of 10 min was allowed to prevent
192 backflow of tracer up the injection track. Before recovering from anesthesia, rats received
193 0.4 mg/kg i.p. ketorolac (Apotex, Mexico) and 50 mg/ kg i.p. ceftriaxone (Kendric, Mexico) to
194 reduce pain and risk of infection. This therapeutic scheme was repeated once per 24h for
195 three consecutive days. Three weeks after the FG injections, the rats were perfused (*vide*
196 *supra*). Free floating coronal sections were obtained with a vibratome. AVP
197 immunofluorescence reaction was made using rabbit anti-AVP antibody as described above.
198 Observations were made using a Zeiss LSM 880 confocal microscope. FG was observed by
199 using a UV excitation filter, and images were artificially assigned a green color for better
200 visualization.
201
202 2.6 Golgi-Cox impregnation and neuronal 2-D reconstruction
203
204 For the argentic impregnation, four 300g male rats were deeply anaesthetized and
205 decapitated. Coronal blocks approximately 5 mm thick, containing the hypothalamus, were
206 cut with a sharp blade and briefly rinsed with PB 0.1M. Blocks were immersed in sequential
207 impregnation A/B and C solutions as indicated in the FD Rapid GolgiStain Kit (FD
208 Neurotechnologies, Ellicott City, MD), during the following two weeks, after which 150 µm
209 coronal sections containing the NLOT and SON were obtained using a vibratome with the
210 cutting chamber filled with solution C, and mounted on gelatin-coated microscope slices,
211 dried overnight at room temperature in the dark and stained with solution D/E. Slices were
212 then washed, dehydrated, cleared with xylenes and cover-slipped with Permount Mounting
213 medium (Fisher Medical, UN1294). Neurons that were identified with more complete
214 somatic/neurite impregnation at SON and NLOT were reconstructed in a 2-D plane using a
215 *camera lucida* attachment mounted on the Nikon Eclipse 50i at 40X magnification.
216
217 2.7 Intracerebral cannula implantation
218
219 For implantation of permanent guide cannula into the NLOT, rats were anaesthetized with a
220 mixture (1:1) of xylazine (20 mg/ml, Procin, Mexico) and ketamine (100 mg/ml, Inoketam,
221 Virbac, Mexico) administered at a dose of 1 ml/kg body weight intraperitoneally. Rat was
222 placed in a stereotaxic frame (Kopf Instruments, Tujunga, CA, USA). Body temperature was
223 maintained at 37 °C using a CMA/150 temperature controller (CMA/Microdialysis,
224 Stockholm, Sweden). Bilateral stainless-steel 26 gauge cannula (C315G, Plastics One,
225 Roanoke, VA, USA) were implanted (stereotaxic coordinates: antero-posterior -1.4 mm,
226 medio-lateral ± 3.2 mm from bregma, and dorso-ventral -8.6 mm from the skull surface.

227 Guide cannulae were affixed on the skull with stainless steel screws and dental acrylic
228 cement (Laboratorios Arias, México City, Mexico) and sealed with dummy cannulae (C315DC,
229 Plastics One). Ketorolac and ceftriaxone were administered as mentioned above for three
230 days following the surgery. Animals were housed in individual cages and allowed to recover
231 from the surgery for one week. Beginning after the 2nd week post-surgery, rats were handled
232 once daily for 5 min for three consecutive days. Rats with fallen cannulae, signs of infection,
233 or altered motricity were excluded from behavioral tests.
234
235 2.8 Social behavior assessment and neuronal activation after intracerebral drug
236 administration
237
238 Behavioral testing was performed on day 11 post-surgery. On the day of the experiment, four
239 experimental groups with rats meeting the selection criteria (*vide supra,* n=20, N=80) were
240 formed and rats were administered the following drugs: control (0.9% NaCl); AVP (1 ng AVP
241 (Sigma V9879, USA)); AVP + V1a antagonist (1 ng AVP +30 ng Manning compound (Bachem,
242 USA)) or AVP + V1b antagonist (1 ng AVP + 10 ng SSR149415 (Axon Medchem, Groeningen).
243 The doses used here were those previously reported [9].The substances were injected
244 bilaterally using two microdialysis pumps (CMA/Microdialysis, Stockholm, Sweden) in a
245 volume of 250 nl over five minutes, and the cannulae were kept in place for 1 min after the
246 injection to prevent backflow and to allow for diffusion as described previously [26].
247
248 Social behavior assessment using the 3CST was started 15 min after microinjections,
249 and the time spent in the social compartment of the 3CST and the number of approaches to
250 the rat *stranger* were quantified as above mentioned during a test period of 10 minutes. Five
251 rats from each experimental group were randomly chosen and perfused after 60 minutes of
252 the 3CST, and FOS immunohistochemistry was performed as described above. The number
253 of Fos positive nuclei in NLOT and structures known to be downstream targets of NLOT were
254 counted within an area of 0.2 mm^2. The rest of the rats were sacrificed with an overdose of
255 pentobarbital and guillotined. Brains were dissected and postfixed for canula location
256 assessment. Scores of rats whose canula tips were placed beyond 200 µm from the perimeter
257 of the NLOT were excluded.
258
259 2.9 RNAscope dual ISH assays
260
261 Rats were transcardially perfused with 4% paraformaldehyde (PFA) in 0.1M PBS (PBS tablets
262 Sigma P-4417). Brains were immediately frozen in 2-methylbutane (isopentane, Sigma-
263 Aldrich, cat 277258, MO, USA) cooled in powdered dry ice, sectioned at a thickness of 12 µm,
264 and mounted onto *Fisher Super Frost slides*. Sections were dried for one hour at 60ºC, then

265 treated with 1X target retrieval reagent (from 10x stock solution provided by the supplier) in
266 a boiling water bath for 5 min. Digestion with Protease-plus was carried out for 15 minutes.
267 The RNAscope duplex method for dual ISH hybridization was performed with RNA probes to
268 identify colocalization of PACAP (probe Rn Adcyap1) with V1b receptors (probe Rn-Avpr1b),
269 V1a receptors (probe Rn-Avpr1a), VGLUT1 (probe Rn Slc17a7), and VGLUT2 (probe Rn
270 Slc17a6) in the NLOT and hippocampus CA2, as well as the colocalization of PACAP receptor
271 1 (probe RN Pac1) and VGLUT1 (Slc17a7) in the insular and gustative cortex. Probes were
272 designed and provided by Advanced Cell Diagnostics (Hayward, CA, United States).
273 Amplification and staining steps were performed following the RNAscope®2.5 HD Assay
274 Duplex protocol for fixed frozen sections.
275
276 2.10 Statistical analysis
277
278 Results are expressed as means ± SEM. D'Agostino and Pearson test was used to evaluate
279 the normality of the data. Differences between means were evaluated by Student's t-test to
280 compare behavior and Fos expression in the water deprivation experiments. One-way
281 ANOVA followed by Dunnet´s multiple comparisons test was used to compare the effects of
282 pharmacological micro-infusion of AVP and combined infusion with its antagonists on social
283 behavior and Fos. Significance in all tests was set at * $p<0.05$, ** $p< 0.01$ and *** $p<0.001$.
284 All statistical analyses were computed using Prism (GraphPad Software, Version 9, San Diego,
285 CA).
286 3. RESULTS
287
288 3.1 WD48 increased the time in the social chamber and number of approaches to the rat
289 *stranger* during the social interaction test (3CST)
290
291 We have previous observed that WD48 increases conditional anxiety (internal, homeostatic,
292 threat) evaluated by elevated plus maze [27] but reduces freezing behavior and increases
293 escaping attempts when rats are exposed to a predator [3]. In both cases, it seems there is a
294 crucial involvement of the hypothalamic vasopressinergic ascending system, but in a
295 *differential circuit involvement, depending on the adversity the animal is facing,* for instance,
296 projections to central amygdala in the conditional anxiety test [6] and projections to lateral
297 habenula in the escaping test [28]. From these observations, the question of social interaction
298 consequences of osmotic challenge, and its circuit involvement, arose. We devised a simple
299 social interaction test, the 3CST (Fig. 1A, for details see section 2.2), to evaluate if the up-
300 regulation of the hypothalamic AVPMNN system could influence social behavior. Water-
301 deprived rats showed a significant enhancement in time spent in the *social* chamber where
302 a rat *stranger* was located withing a wire cage (Fig. 1B, right) (control: 215.5 ±31.66 vs. WD48:

350.3 ±32.38; p<0.01) and in the number of approaches/sniffing to the rat *stranger* (control: 7.33 ±0.91 vs. 24h WD: 11 ±0.81; p<0.01) (Fig. 1B, left).

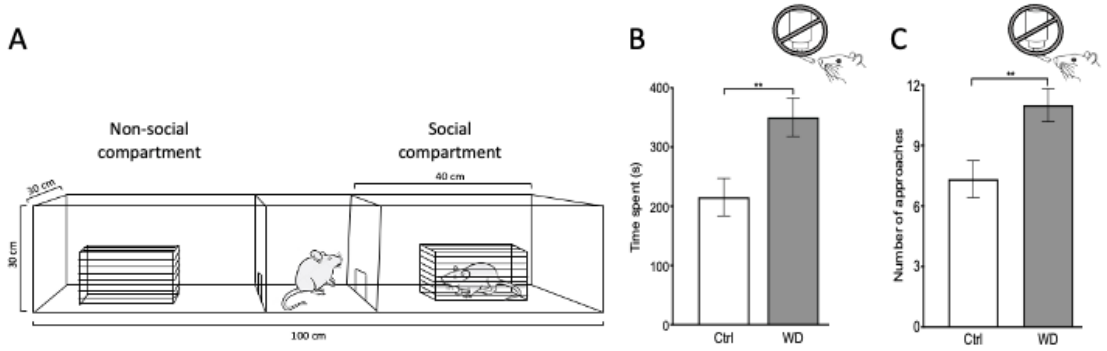

Figure 1. Water deprivation during 48h (WD48) increased the time of social interaction. A*: schematic representation of the three-chamber social test (3CST) used during sociability evaluations.* ***B: (left****) WD48 led a significant increase of the time spent in the social chamber where the rat stranger was kept inside a wire cage as compared control rats.* ***B: (right****) WD48 increased the number of approaches/sniffing to the rat stranger compared to the control group. Results are expressed as means ± SEM. Ctrl n= 12, WD n= 14. ** p < 0.01. Unpaired Student´s t test.*

3.2 Fos expression triggered by WD48+3CST compared with basal, WD48 or 3CST alone reveals a social behavioral neuronal network

Fos expression analysis is a powerful approach for obtaining insight into patterns of neuronal activation during internal/external stimulation and behavioral adaptation. To investigate Fos activation, experimental subjects were submitted to one of four conditions: 1) basal condition, with food and water *ad libitum* and un-disturbed before perfusion/fixation; 2) WD48, with food *ad libitum* (usually food intake ceases after 12h of water deprivation), un-disturbed before perfusion/fixation; 3) food and water *ad libitum*, subjected to 3CST - the perfusion/fixation was performed 60min after the end of the test; 4) WD48 prior to 3CST - the perfusion/fixation was performed 60 min after the end of the test. We systematically examined increased Fos expression, as a measure of neuronal activation, throughout the brain in these four groups and performed semi-quantitative assessment of Fos elevation (Table, and see the analysis criteria in section 2.4).

As expected, social interaction caused moderate to large increases in Fos expression in regions involved in processing of exteroceptive and interoceptive information. These regions include those involved in olfactory processing such as the anterior olfactory nucleus,

333 accessory olfactory bulb, nucleus of the lateral olfactory tract, piriform and entorhinal cortex,
334 taenia tecta, cortical and posterior amygdala, olfactory tubercle, and endopiriform nucleus
335 [29, 30]; regions involved in visual processing such as the primary and secondary visual cortex,
336 pretectal nucleus, the lateral geniculate complex of the thalamus and the midbrain nucleus
337 of the posterior commissure [31]; regions involved in auditory processing such as the inferior
338 colliculus, medial geniculate nucleus and basolateral amygdala [32]; limbic regions that
339 participate in the integration of emotional states such as central amygdala, bed nucleus of
340 the stria terminalis, accumbens, ventromedial hypothalamus and septum; regions involved
341 in memory and coding of space information such as the hippocampal formation, entorhinal
342 cortex and retrosplenial cortex [33, 34]; and hypothalamic nuclei involved in stress, aggression,
343 and arousal regulation such as the paraventricular and ventromedial hypothalamic nuclei.
344 In contrast, activation of neurons by water deprivation was dramatically greater in
345 SON, and PVN, two nuclei rich in osmosensitive AVPMNNs, whereas the SCN, containing non-
346 osmosensitive vasopressinergic neurons, and other non-vasopressin-expressing nuclei of
347 brain, exhibited far less activation in response to water deprivation (Table 1). A high number
348 of Fos positive nuclei was found in the BNST, a region reported to be targeted by projections
349 from osmosensitive glutamatergic neurons of the subfornical organ [35, 36]
350
351 WD48+3CST-induced spatial neuronal activation pattern coincided with the main
352 efferent regions of SON and the nucleus of the lateral olfactory tract (NLOT). Among brain
353 regions showing neuronal activation (Fos expression) specifically associated with *combined*
354 WE48 and 3CST exposure, the NLOT was of particular interest, since this region contains
355 vasopressinergic fibers which were visibly increased by WD48 (Figure 2). The main efferent
356 cortical regions of NLOT (see Allen mouse interaction map, Adcyap1-2A-Cre, Exp.
357 187269162, and Fig. 5A) also showed strong increase of Fos expression after WD48+3CST.
358 These regions include anterior olfactory nucleus, piriform cortex, agranular insular cortex,
359 gustatory cortex, dorsal insular cortex, basolateral amygdala, claustrum, and endopiriform
360 nucleus (see Table, bold lettered regions).
361
362 3.3 Forty-eight hours of water deprivation (WD48) potentiated hypothalamic
363 vasopressinergic system and activated Fos in neighboring NLOT
364
365 We examined further the source of origin of vasopressinergic fibers, as well as the nature of
366 Fos-positive cells in NLOT after water deprivation. Concordant with progressive activation of
367 secretion of AVP from posterior pituitary (Fig. 2A) following water deprivation, there was an
368 increase in Fos expression both in PVN and SON (Fig. 2B'), as noted in Table, and in NLOT as
369 well (Fig. 2B). Furthermore, AVP-positive terminals were found in close apposition to Fos-
370 positive cells in NLOT (Fig. 2B´´), and the intensity of vasopressin terminals in NLOT was

371 correspondingly increased (Fig. 2C vs. 2D). Thus, it appeared that upregulation of the
372 vasopressinergic system by osmotic stress facilitated an increase in the number and/or
373 intensity of staining of AVP fibers in the NLOT.

Table 1. Semi-quantitative assessment of neural activation in 4 experimental conditions

Region	Abs.	Control	Social Interaction	48h WD	48h WD Social Inter.
Cortical plate (CTXpl)					
Anterior cingulate cortex	AC	-	++	+	++
Main olfactory bulb	MOB	-	-	+	+
Accessory olfactory bulb	AOB	-	++	-	++++
Agranular insular	**AI**	**-**	**++**	**+**	**+++**
Anterior olfactory nucleus	**AON**	**-**	**+++**	**++**	**++++**
CA1 (dorsal hippocampus)	CA1d	+	+	+	+
CA1 (ventral hippocampus)	CA1v	-	++	+	+++
CA3 (temporal hippocampus)	CA3t	-	++	-	++
CA2 (dorsal hippocampus)	CA2d	-	++	-	++
Dentate gyrus	DG	+	++	++	++*
Ectorhinal area	ECT	-	++	+	++++
Entorhinal area	ENT 4	-	++	+	+++
Gustatory cortex	**GU**	**-**	**+**	**+**	**+++**
Infralimbic cortex	ILA	-	++	-	+++
Nucleus of the lateral olfactory tract	**NLOT**	**-**	**++**	**+**	**++++**
Orbital cortex	ORB	-	++	+	+++
Pos-subiculum		-	+	-	++
Para-subiculum	PAR	-	-	-	+
Piriform amygdalar cortex	PAA	-	+	-	++
Piriform cortex	**PIR**	**-**	**+++**	**+**	**++++**
Prelimbic cortex	PL	-	++	-	++
Presubiculum	PRE	-	+	-	+++
Retrosplenial cortex	RSP2/3	-	+++	-	++++
Somatomotor cortex, L5	MO5	-	+	-	++
Somatosensory cortex, L2/3	SS2	-	++	-	+++
Somatosensory cortex, L5/6	SS5	-	++	-	+++
Subiculum	SUB	-	-	+	+
Taenia tecta	TT	-	+++	-	+++
Visual primary cortex L2/3	V-2/3	-	+++	-	++++
Visual primary cortex L6	V1 -6	-	+++	-	+++
Visual secondary cortex	V2	-	+++	-	++++
Cortical subplate (CTXsp)					
Basolateral amygdalar nucleus	BLA	-	++	+	+++
Basomedial amygdalar nucleus	BMA	-	+	-	+
Cortical Amygdala	COA	-	+	+	+
Claustrum	**CLA**	**-**	**++**	**+**	**+++**
Endopiriform nucleus	**EPd**	**-**	**+++**	**+**	**++++**
Lateral amygdala	LA	-	+	-	+
Posterior amygdalar nucleus	PA	-	++	+	++
Hilus (dentate gyrus)	HYL	+	+	-	+
Cerebral nuclei (CNU)					
Bed nuclei of stria terminalis	BST	-	+++	+++	++++
Caudate putamen	**CP**	**-**	**+**	**+**	**+++**
Globus pallidus	GP	-	+	-	++
Central amygdalar nucleus	CEA	-	++	++	+++
Diagonal band nucleus	NDB	-	+++	++	++++
Lateral septum	LS	-	++	+	+++
Medial amygdalar nucleus	MEA	-	++	-	+++
Nucleus accumbens	**ACB**	**-**	**++**	**+**	**+++**
Olfactory tubercule	**OT**	**-**	**++**	**++**	**++**
Pallidum ventral	PAL	-	+++	+	+++
Sustancia inominata	SI	-	+	+	+

Region	Abs.	Control	Social Interaction	48h WD	48h WD Social Inter.
Interbrain (IB)					
Anterior hypothalamic nucleus	AHN	+	++	+	++
Arcuate hypothalamic nucleus	ARH	+	+	++	+++
medial geniculate	mGd	-	+	-	+
Dorsal lateral geniculate	LGd	-	++	-	+++
Dorsomedial hypothalamic nucleus	DMH	+	++	+	+++
Intergeniculate leaflet of the lateral geniculate complex	IGL	-	++	+++	++++
Lateral dorsal nucleus of the thalamus	LD	-	++	+	++
Lateral habenula	LH	-	+	++	+++
Lateral hypothalamic area	LHA	-	++	++	++++
Lateral preoptic area	LPO	-	+	+++	++++
Medial geniculate	MG	-	++	-	++
Medial habenula	MH		++	-	+++
Medial preoptic area	MPO	-	+	++	++
Nucleus of reuniens	RE	+	++	++	++
Paraventricular nucleus hypothalamus	PVH	++	++	+++++	+++++
Paraventricular thalamus	PVT	+	+	+	+++
Periaqueductal gray	PAG	-	+	+	+++
Posterior hypothalamic nucleus	PH	+	++	++	+++
Premammillary	PM	-	++	+	++++
Reticular nucleus of the thalamus	RT	+	++	+	++
Subthalamic nucleus	STN	+	++	+++	+++
Suprachiasmatic	SCH	+	+	+	+++
Supramammillary nucleus	SUM	-	+	++	+++
Supraoptic nucleus	SON	-	+	+++++	+++++
Ventromedial hypothalamic nucleus	VMH	-	+++	+++	++++
Zona incerta	ZI	+	++	++	+++
Midbrain (MB)					
Anterior pretectal nucleus	APN	-	+++	+	++++
Dorsal raphe nucleus	DR	-	++	+	+++
Inferior colliculus	IC	+	+++	++	+++
Midbrain reticular nucleus	MRN	+	+	+	++
Nucleus of the posterior commissure	NPC	+	+++	+	++++
Pretectal area	PRT	-	++	++	+++
Substantia nigra, compacta	SNc	-	++	++	+++
Substantia nigra, reticular	SNr	-	++	++	+++
Superior colliculus	SC	+	+	+	++
Ventral tegmental area	VTA	-	++	++	++
Hindbrain (HB)					
Parabrachial nuclei	PBN	-	++	+	++
Pontine reticular nucleus	PRN	-	++	+	++

Fos + nuclei were evaluated in a 0.2 mm^2 area and the following scores were assigned: (-) no Fos+ nuclei observed; (+) 1-25; (++) 26-50; (+++) 51 – 75, (++++) 76-100 and (+++++) >100.

374
375

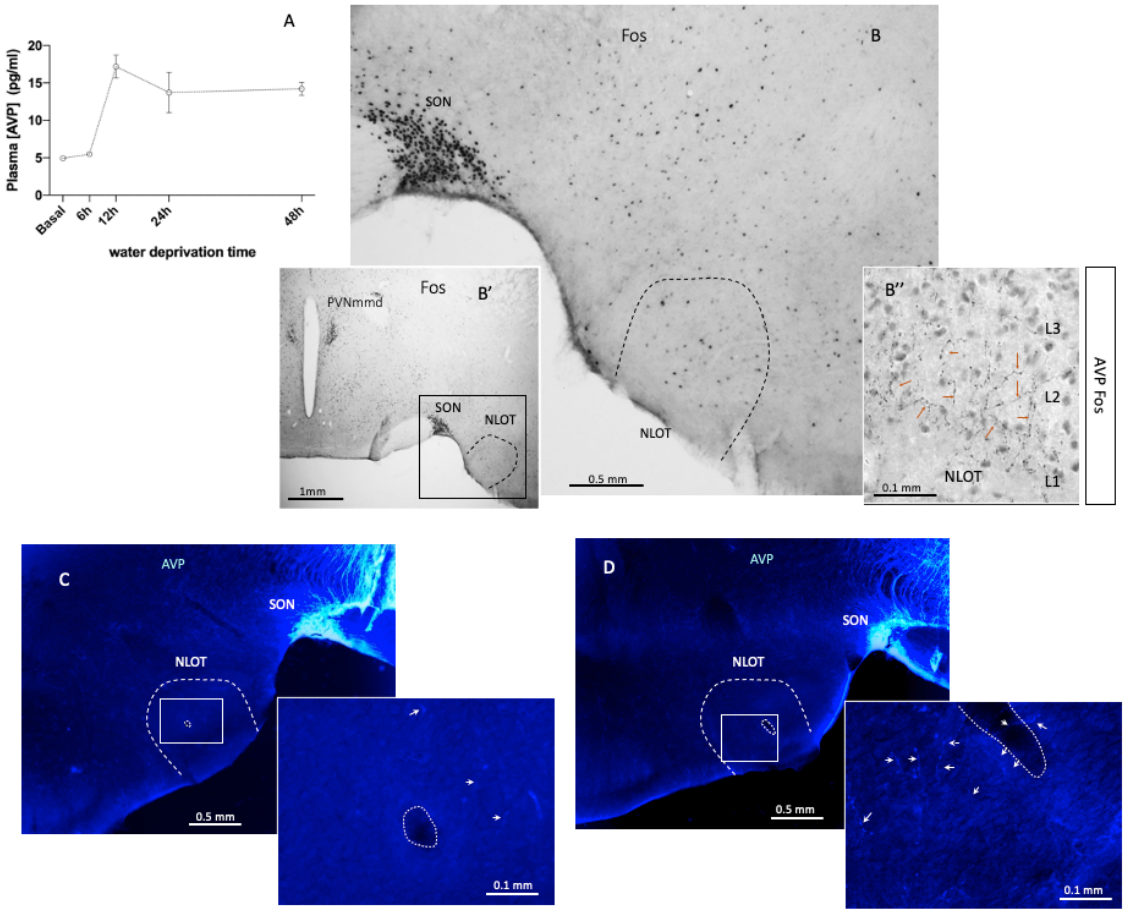

Figure 2: Forty-eight hours of water deprivation (WD48) potentiated hypothalamic vasopressinergic system and activate Fos in neighboring *NLOT. A: Time course of dynamic changes in plasma arginine vasopressin (AVP) concentration during 48 h of water deprivation, measured in wild-type male rats (n=5) with ELISA (modified from Zhang et al, 2020, with permission). Bs: example of Fos expression in hypothalamus at supraoptic level and cortical amygdalar region (B': low magnification of B and B'', Fos and AVP IHC in NLOT after WD48). C and D: photomicrographs showing AVP immunoreactivity (ir) (digital photos in negative mode to enhance AVP immunopositive fibers' visibility) in the same region of B, in control and WD48 rats. Note in the high magnification insets that after WD48, the AVP + fibers clearly increased their visibility (white arrows). A vessel within the magnified region is indicated in dotted lines for anatomical reference. Abbreviatures: PVNmmd: paraventricular nucleus, medial magnocellular division; SON: supraoptic nucleus; NLOT: nucleus of lateral olfactory tract*

<u>3.4 Vasopressinergic input to NLOT from SON of the hypothalamus revealed by Fluoro-Gold (FG) retrotracing and Golgi-Cox stained sample analysis</u>

Retrograde tracing in conjunction with staining for AVP was employed to demonstrate that SON AVPMNNs project to NLOT. Iontophoretic FG injection targeted to NLOT (see section 2.5) resulted in strong labeling in SON (Fig. 3A and B). Most of the labeled cells were immunopositive for AVP (Fig. 3B). Microscopical observation of Golgi-Cox stained samples of brain coronal sections (150 µm of thickness), containing NLOT and the SON, with only sparse staining (Fig. 3C and 3D), revealed that SON magnocellular neurons could give rise to as many as three main axons which coursed medial, lateral and dorsally. Figure 3Da and 3Db show two magnocellular neurons, single-stained. Those two cells are designated as cells "a" and "b" in Figure 4. Each of the cells emitted three main axons, numbered 1, 2, and 3, which coursed medial, dorsal and laterally. Fig. 3Dc shows the axon coming from cell "b", axon #3, with a huge varicosity, a characteristic of the magnocellular neurons, entering layer 1 of NLOT (Fig. 4F)

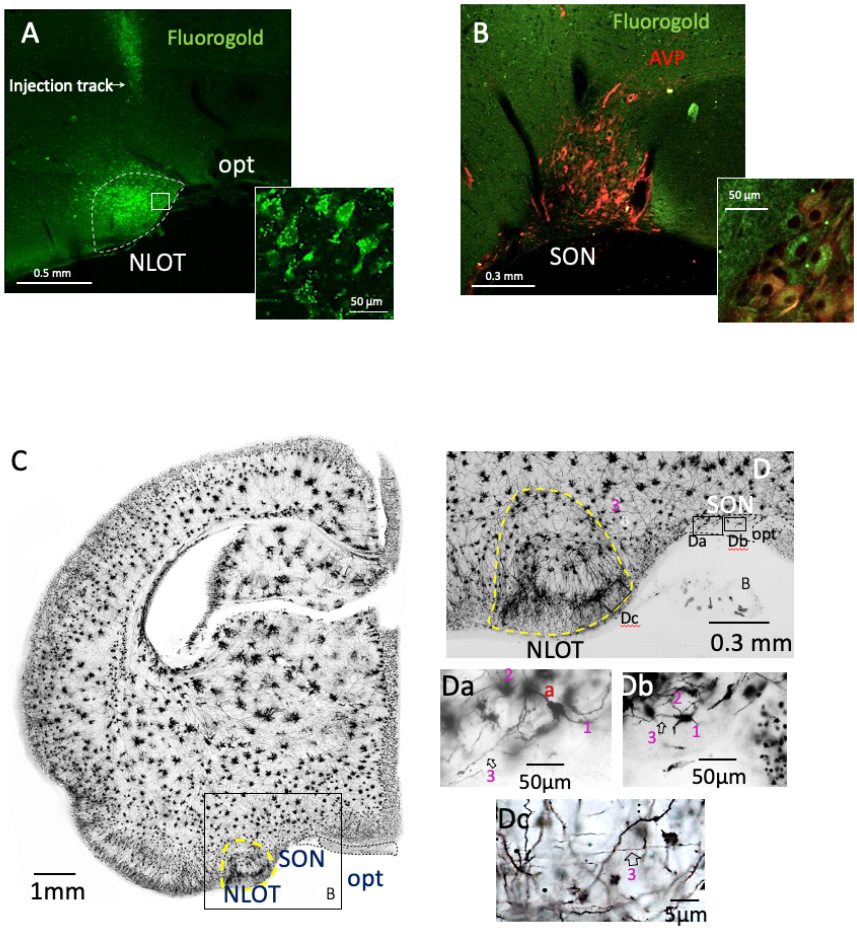

Figure 3. ***Anatomical relationship and interconnections between rat hypothalamic supraoptic nucleus (SON) and the nucleus of lateral olfactory tract (NLOT).*** *A and B: retrograde tracer fluorogold injected to NLOT labeled the SON vasopressin immunoreactive neurons. C. Golgi-*

412 *Cox staining of the rat brain coronal section (150 µm of thickness) containing NLOT and the*
413 *SON. D: higher magnification of C with squared region with NLOT and SON showed. Note the*
414 *clearly visible allocortical feature, three layers of the NLOT clearly visible. Da and Db show*
415 *two magnocellular neurons, single-stained within the SON, that they emitted 3 main axons*
416 *from soma or proximal dendrites and coursed medially (1), dorsally (2) and laterally (3) that*
417 *could be followed and reconstructed using adjacent sections (see Fig. 4A). Dc: showing the*
418 *axon coming from cell "b", axon #3, with huge varicosity, which is a characteristic of the*
419 *magnocellular neurons, entering the layer 1 of NLOT, could be followed in the two adjacent*
420 *sections. Hollow arrows indicate the main axons coming out from the magnocellular cells a*
421 *or b.*
422
423 3.5 Molecular signature of NLOT principal neurons (layer 2, NLOT2) and projection fields
424 reveals a cooperative role between hypothalamic vasopressinergic signaling and an NLOT
425 PACAPergic neuronal population
426
427 The NLOT is an isolated tri-laminar ovoid cell mass located in the anterior cortical amygdalar
428 region [19, 37]. Nissl staining reveals three cell layers within the NLOT nucleus. Layer 1 (NLOT1)
429 is a subpial molecular zone with scattered neurons, which receives mitral cell input from the
430 main olfactory bulb. Layer 2 (NLOT2) is a thick and dense corticoid aggregate of pyramidal
431 neurons of medium size with apical dendrites entering NLOT1 (Fig. 4F, for example). Layer 3
432 (NLOT3) is a multiform layer disposed more deeply than layer 2. It contains a mixture of small
433 and large neurons, some of them possibly representing inhibitory interneurons of subpallial
434 origin [21]. We next explored the neurochemical signature(s) of the neurons in NLOT that are
435 the presumptive targets of vasopressinergic terminals from SON, which terminate mainly in
436 the layer 1 where the pyramidal neurons apical dendrites branch. Figure 4A shows three
437 types of neuronal morphology reconstructed using camera lucida and Golgi-Cox stained
438 samples (section thickness: 150 µm). Pyramidal neurons of the NLOT2 are of particular
439 interest here. Using dual ISH (RNAscope duplex method), we identified a population of
440 PACAPergic, VGLUT1 and VGLUT2 expressing neurons in layer II of NLOT (Fig. 4C and 4D) [38]
441 representing pyramidal neurons (black cells) which, upon Golgi staining and reconstruction,
442 send dendritic processes into both layer I and layer III of NLOT where the SON magnocells
443 send their axons (Fig. 4A, red axons reconstructed with camera lucida in three adjacent
444 sections of thickness 150 µm each). As these neurons also express the vasopressin receptors
445 V1a and V1b (Fig. 4E and 4F), they are candidate target neurons of the vasopressinergic
446 projections from SON. In fact, these PACAPergic (and glutamatergic) neurons are also those
447 that exhibit Fos elevation after 48WD.
448

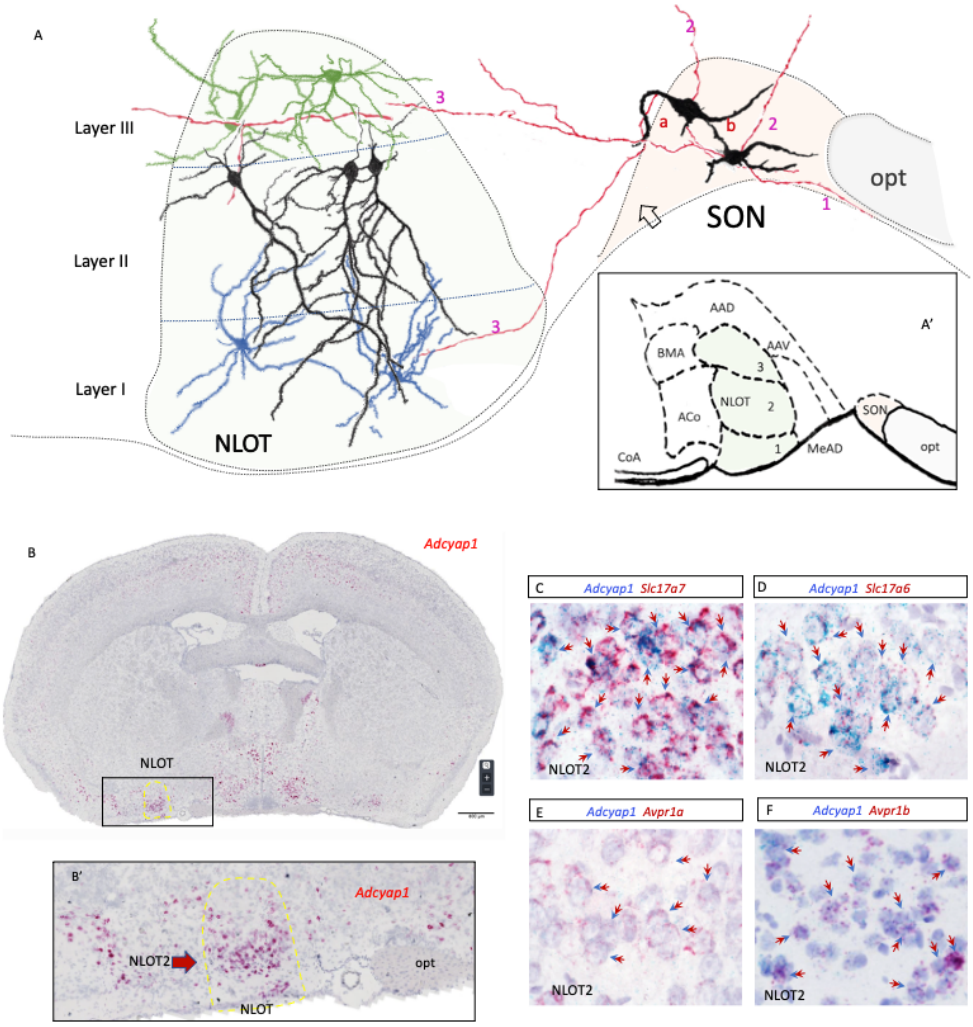

Figure 4. ***Molecular signature of NLOT principal neurons (layer 2, NLOT2), glutamatergic, PACAPergic and V1a and V1b mRNA expressing.*** *A: coronal section showing the RNAscope ISH for Adcyap1, mRNA encoding PACAP, at the nucleus of lateral olfactory tract (NLOT) antero-posterior level. The NLOT strongly expresses PACAP mRNA. A': amplification of squared region A. Note that most of PACAPergic neurons are the layer 2 neurons (NLOT2). B-E, dual in situ hybridization (DISH) using RNAscope duplex method showing the PACAPergic neurons of NLOT2 co-express Slc17a7 (mRNA for VGLUT1), Slc17a6 (mRNA for VGLUT2), Avpr1a (mRNA for vasopressin receptor V1a) and Avpr1b (mRNA for vasopressin receptor V1b). Doble arrows indicate examples of co-expression. F: camera lucida reconstructions of selective NLOT neurons, from Golgi-Cox-stained sample of Fig. 2C. Note the NLOT2 neurons (black neurons) are mainly pyramidal neurons with the apical dendrites and their subsequent branching toward the layer 1 and the brain ventral surface where most of AVP immunopositive fibers were observed. Blue cells were camera lucida-reconstructed from the NLOT1 and green cells from the NLOT3. Two SON (light beige shading magnocellular neurons with three axons emitted from cell bodies or proximal dendrites, followed in the two adjacent sections. "1" indicate the axons coursing toward the infundibulum, "2" indicate the axon coursing dorsally and "3" indicate axons coursing laterally toward NLOT (light green shading) and cortical amygdala (CoA).*

Cortical efferent regions of NLOT2 PACAPergic pyramidal neurons which also express VGLUT2 [38] (Fig. 4D) and the transcription factor Sim1 [39] are revealed within the Allen connectivity atlas (Fig. 5A and supplementary Fig. 1). Figure 5A depicts a map of NLOT projections made with a mouse line Adcyap1-2A-Cre, Exp. 187269162, injected with a Cre-dependent AAV tracer into the NLOT that expresses EGFP. The main efferent regions include anterior olfactory nucleus, piriform cortex, agranular insular cortex, gustatory cortex, dorsal insular cortex, basolateral amygdala, claustrum, and endopiriform nucleus (see Table, bold lettered regions) which all strongly express the PACAP receptor PAC1 mRNA (Adcyap1r1, Fig. 5B) and also co-express VGLUT1 mRNA (Slc17a7, Fig. 5C and insets).

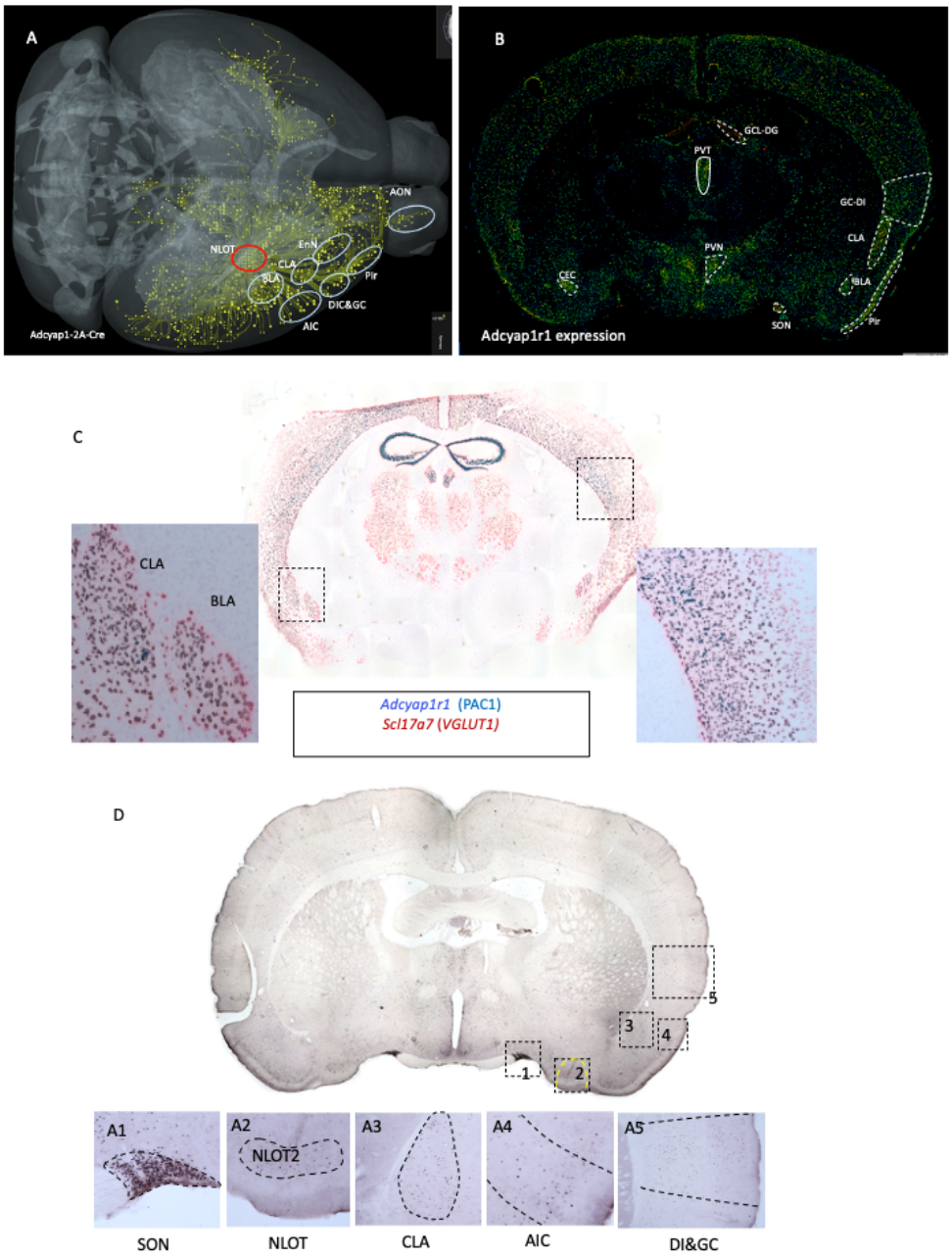

476 ***Fig. 5 Glutamate-PACAPergic NLOT main efferent regions analyzed in this study strongly co-***
477 ***express mRNAs of PACAP receptor PAC1 (Adcyapr1r) and VGLUT1 (Slc17a7) and were***
478 ***activated by 48WD.*** *A: Axonal projections from PACAP transfected NLOT neurons. Obtained*
479 *from Allen mouse brain connectivity atlas (Experiment: 187269162 Transgenic line: Adcyap1-*
480 *2A-Cre injected into NLOT with an AAV Cre-dependent vector). B: coronal section showing the*
481 *expression of Adcyap1r1 (PAC1 receptor mRNA) with cortical regions that are target of NLOT*
482 *are delineated in dotted lines. Image obtained from Allen ISH brain atlas (Experiment:*
483 *74988667) C: Coronal section processed for dual ISH using Duplex RNAscope, to show the*
484 *colocalization of VGLUT1 and PAC1 in cortical regions targeted by projections from*
485 *PACAPergic NLOT neurons. D: Coronal section showing Fos expression after WD48+3CSI.*
486 *Panels: D1 – D5 show the key regions discussed in this study: SON: supraoptic nucleus; NLOT:*
487 *nucleus of lateral olfactory tract; CLA: claustrum; AIC: Agranular insular cortex; DI, dorsal*
488 *insular cortex; GC: gustatory cortex . The whole brain Fos expression semi-quantitative*
489 *analysis is reported in table 1.*
490
491 <u>3.6 Increased social behavior and Fos expression induced by vasopressin micro-infusion in</u>
492 <u>NLOT is blocked by both V1a and V1b receptor antagonists</u>
493
494 In order to ascertain whether or not AVP can directly modulate neuronal activity in NLOT,
495 and influence social behavior, AVP (1 ng/side) was bilaterally infused into this region (Fig. 6A)
496 15 min before 3CST. To evaluate the participation of the V1b and V1a receptors, the
497 pharmacological antagonists SSR149415 (V1b antagonist) and Manning compound (V1a
498 antagonist) were co-injected with vasopressin at 30 ng/side in 20 rats per condition. All
499 cannula tips of the animals included in the behavioral or Fos analysis were shown to be within
500 a 200 µm perimeter of the NLOT boundaries
501
502 The microinjection of AVP significantly increased the time (350.34 ±21.3, $p<0.01$) that
503 the experimental rats spent in the *social* compartment as compared with the saline-treated
504 group (215.4 ±16.92). This effect was reduced to control level vasopressin injection was
505 accompanied by co-administration with SSR149415 (256.26 ±40.32) or Manning compound
506 (156.3 ±29.57)(Fig. 6C, right). A significant elevation in social approaches was seen after
507 intra-NLOT infusion of AVP (11.92 ±2.15) in comparison to the saline group (5.81 ±0.75;
508 $p<0.001$). The co-infusion of AVP+ SSR149415 prevented the increase in the number of
509 approaches to the social compartment (6.35 ±0.51) seen with AVP alone, showing a similar
510 value to the saline group (Saline: 5.81 ±0.75). Microinfusion of Manning compound along
511 with AVP similarly decreased the number of approaches (8.00 ±1.03) compared to AVP alone
512 (Fig. 6C, left).
513

To confirm that NLOT PACAPergic/glutamatergic neurons are plausible targets for activation by vasopressin projections from SON, we examined Fos elevation in selected regions known to be involved in social behavior (Fig 6D). One-way ANOVA followed by Dunnett multiple comparison test showed that bilateral AVP (1 ng/side) infusion into the nucleus of the lateral olfactory tract (NLOT) elicited an increase of Fos+ expression in NLOT compared to saline (saline: 27.20 ±0.97, vs AVP: 44.00 ±2.21, $p<0.0001$), no significant differences were observed between saline and AVP+SSR149415 (26.60 ±3.37), nor between saline vs. AVP + Manning compound (26.80 ±1.35). In the anterior olfactory nucleus (AON) we found that compared to saline (40.80 ±2.45), AVP increased the number of Fos positive nuclei (68.40 ±1.53, $p<0.001$), and compared to control, there was a significant decrease in the number of Fos positive nuclei after co-infusion of AVP+SSR149415 (24.2 ±1.93, $p<0.0001$) or AVP + Manning compound (22.60 ±2.01, $p<0.0001$). In the basolateral amygdala (BLA), AVP infusion into NLOT elicited significant increases in Fos activation compared to saline infusion (saline: 26.00 ±1.87 *vs. AVP:* 41.00 ±2.91, $p<0.001$) and the effect of AVP infusion was blocked with AVP+SSR149415 (24.00 ±1.87) and with Manning compound (22.00 ±2.55). NLOT AVP infusion increased the number of Fos+ nuclei in agranular insular cortex (AI) compared to saline (saline: 5.00 ±0.70 vs. AVP: 26.60 ±1.50; $p<0.0001$). While the effect of AVP antagonists on AVP was not as complete here as in other areas (AVP+SSR149415: 18.4 ±0.81, AVP + Manning compound: 15.8 ±1.35, $p<0.01$). In gustatory area (GU), compared to control, AVP infusion into NLOT significantly increased the number of Fos+ nuclei (Saline: 12.60 ±1.32 *vs. AVP:* 76.60 ±7.43, $p<0.0001$) and V1a and V1b antagonists abolished this

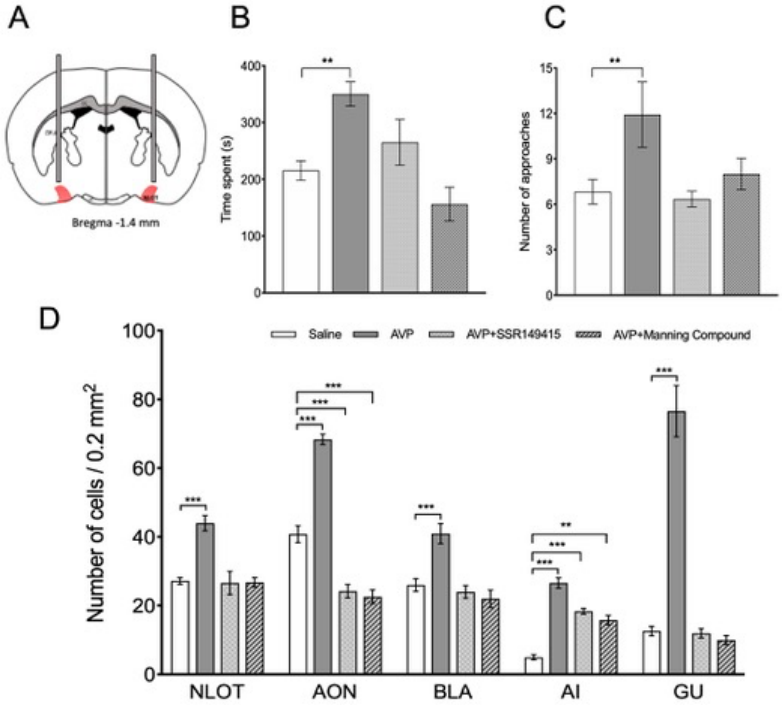

535 effect as no differences were found between saline and SSR14915 (12.00 ±1.37), or Manning
536 compound (10.00 ±1.30)(Fig. 6D).
537
538 ***Figure 6. Vasopressin microinfusion into the nucleus of the lateral olfactory tract (NLOT)***
539 ***induces both an increase in social behavior and Fos+ nuclei expression****. (**A**) Representative*
540 *scheme showing a bilateral cannula placeman within the NLOT. (**B**) AVP infusion (1ng/side)*
541 *increased the time that the rats spent inside the social compartment these effects were fully*
542 *prevented by the simultaneous infusion of both AVP V1b receptor (10 ng/side, SSR149415*
543 *(SSR) antagonist, and AVP V1a receptor (10 ng/side, Manning compound antagonist. (**C**) A*
544 *significant difference was found in the number of entries between the infusion of AVP vs the*
545 *saline group these effects were blocked by the simultaneous infusion of AVP V1b and V1a*
546 *receptor antagonist. (**D**) AVP infusion into NLOT elicited an enhancement of Fos+ expression*
547 *in AON, BLA, AI, and GU, as compared with the respective saline-treated group. The*
548 *simultaneous infusion of AVP+V1b and AVP+V1a antagonist resulted in a decreased Fos*
549 *expression in all the areas studied in this work. Abbs: NLOT: nucleus of lateral olfactory tract;*
550 *AON: accessory olfactory nucleus; BLA: Basolateral amygdala; AI: agranular insular; GU:*
551 *gustatory area. Results are expressed as means ± SEM. **P< 0.01; ***P<0.001. Two-way*
552 *ANOVA followed by Dunnett´s multiple comparisons test was used to evaluate social behavior*
553 *(Saline n=20; AVP n=19; AVP+SSR n=19; AVP+Manning C. n=19) and One-way ANOVA*
554 *followed by Dunnett´s multiple comparisons test to Fos expression (n= 5 rats for each group).*
555
556 DISCUSSION
557
558 In this study, we focused on a newly-characterized projection system from AVPMNNs of the
559 supraoptic nucleus (SON) of the hypothalamus to the nucleus of the lateral olfactory tract
560 (NLOT), the activation of these neurons by water deprivation, and ensuing effects on their
561 neurochemistry, their connections, and their potential effects on social behavior.
562
563 We report here that rats stressed osmotically via WD48 had a higher score in
564 sociability than euhydrated rats. It has been previously reported that osmotic stress potently
565 increases the metabolic activity of AVPMNNS in the hypothalamus, and that increased AVP
566 mRNA expression in PVN and SON correlate with levels of social interaction in mice [40, 41].
567 Intracerebroventricular infusion of AVP increases social contact in prairie voles [42] and novel
568 conspecific social interaction in the Syrian hamster [43]. Brattleboro rats lacking AVP due to a
569 genetic prohormone processing defect, show various behavioral impairments, including
570 altered social development [14] and less social playing and prosocial ultrasonic vocalizations
571 [13]. The duration of social recognition in rats [44] is dependent on the levels of AVP in the
572 lateral septum. Variation in expression of vasopressin receptor genes (AVPR1A, AVPR1B)
573 correlates with variation in social behavior in rhesus macaques [45]. Our novel finding here is
574 the identification of the direct innervation of the NLOT by AVP projections from the SON,

575 which has not been reported in the literature previously and represents a candidate circuit
576 activated by osmotic challenge induced by water deprivation.
577
578 We also observed the displayed increased Fos expression in the nucleus of the lateral
579 olfactory tract (NLOT) and its efferent cortical regions after WD48 + 3CST, indicating that the
580 homeostatic state is able to modulate neocortical social interaction processing centers via a
581 hub within the cortical amygdalar lateral olfactory tract nucleus, NLOT. We confirmed the
582 involvement of AVP within this hub by injecting vasopressin directly into the NLOT. A novel
583 finding in this study was that both V1a and V1b receptor antagonists reduced the AVP-
584 induced increase in sociability. The fact that this phenomenon was blocked by either V1a or
585 V1b receptor antagonists co-infused with AVP suggests that both types of receptor are
586 necessary, and either is insufficient, to mediate these behavioral effects.
587
588 NLOT projects to the accessory olfactory system which is activated during social
589 investigation behavior in which AVP participates through neuronal signaling to filter social
590 cues of odor [(46)]. Similarly, NLOT-lesioned rats spend significantly less time sniffing out odors
591 associated with social contacts than intact rats regardless of the number of times exposed to
592 the olfactory stimulus [(47)]. It is known that water deprivation enhances both AVP-
593 immunoreactivity and Fos expression in the hypothalamic paraventricular and supraoptic
594 nuclei [(5)] and therefore vasopressin effects could be exerted elsewhere than at the level of
595 the amygdala. However, the fact that exogenous administration of AVP into NLOT could
596 produce identical behavioral effects as those induced by WD support the conclusion that the
597 effects of WD are mediated by AVP release in the NLOT. The effects of AVP microinfusion in
598 NLOT on Fos activation in AON, BLA, AI, and GU, and blockade of Fos activation by AVP
599 antagonist co-administration in NLOT alone, is also consistent with the notion that AVP
600 affects activation of this behavioral network by its action as a neurotransmitter at the NLOT
601 'hub'. A previous study documented enhancement of social interaction after osmotic
602 dehydration (subcutaneous injection of 2 M NaCl) [(48)]. It seems likely that this osmotic
603 stressor, like water deprivation, may affect social behavior also through AVP release in NLOT
604
605 It is uncertain at the present time how altered social behavior (increased social
606 interaction) after water deprivation represents an integration of homeostatic and allostatic
607 drive that is beneficial to animal survival (and would, at least simplistically) explain the
608 evolution and stabilization of the pathway described here in mammalian brain. Broadly,
609 increased attention to the behavior and proximity of con-specifics during resource scarcity
610 may have both positive and negative effects. For example the borer and social mutations of
611 another neuropeptide-liganded GPCR, the NPY-like receptor of C. elegans, are posited to
612 drive foraging behavior when food is scarce, and social behavior (and increased mating)

613 when food is plentiful, respectively [49]. In this context, increased sociability during water
614 deprivation would seem to be disadvantageous, rather than the reverse. However, it must
615 be borne in mind that the behavioral model chosen here as a 'behavioral readout' for water
616 deprivation (social interaction) may be insufficiently rich/complex to capture the full range
617 of advantages and disadvantages of increased social interaction during periods of scarcity,
618 and indeed 'water deprivation' may not necessarily model resource scarcity per se. For
619 example, salt preference may be a behavioral characteristic that involves
620 vasopressinergic/dynorphinergic MNNs and helps to integrate water seeking and
621 consumption with salt balance ([2] and references therein). Thus, we postpone speculation
622 on the potential evolutionary advantages of a linkage between social behavior and water
623 deprivation, and note here only that this linkage exists, at least in part, because of a
624 vasopressinergic projection from SON (exclusive of PVN and SCN) to NLOT, in the rat.
625
626
627 Besides the vasopressinergic SON→NLOT PACAPergic projection system described
628 here, there are at least two other AVPMNN systems that link homeostasis and behavior that
629 have been recently reported [3, 6, 28, 50]. In these latter cases, the AVP target neurons (GERNs
630 in LHb, amygdalar neurons, noradrenergic neurons) have their own well-established
631 downstream connections that suggest how vasopressinergic inputs to them ultimately
632 affects behavior. For the present case, i.e. the SON→NLOT pathway, it is much less clear how
633 activation accomplishes enhanced social behavior, because the downstream connections of
634 NLOT2 PACAP/glutamate neurons are not yet well-established.
635
636 As a final note, it is worth remarking that receptor-specific pharmacological
637 manipulation of this pathway (and parallel ones) for potential therapeutic purposes could be
638 easily separate vasopressin-like effects on osmoregulation itself (mediated mainly via V2),
639 from behavioral effects. It will be of interest in future experiments to determine whether or
640 not a combination of V1a and V1b *agonists* can mimic the behavioral effects of AVP infusion
641 into the brain on behavioral independently of osmoregulatory effects intrinsic to arginine
642 vasopressin.
643
644 REFERENCES
645 1. Eiden LE, Hernández VS, Jiang S, Zhang L. Neuropeptides and Small-molecule
646 Amine Transmitters: Cooperative Signaling in the Nervous System. *Cellular and Molecular*
647 *Life Sciences*. 2022, in press.
648 2. Zhang L, Hernández VS, Murphy D, Young WS, Eiden LE. Fine chemo-anatomy of
649 hypothalamic magnocellular vasopressinergic system with an emphasis on ascending
650 connections for behavioural adaptation. In: Valery Grinevich ÁD, ed. *Neuroanatomy of*
651 *Neuroendocrine Systems* Springer-Nature 2021.

652 3. Zhang L, Hernandez VS, Vazquez-Juarez E, Chay FK, Barrio RA. Thirst Is
653 Associated with Suppression of Habenula Output and Active Stress Coping: Is there a Role
654 for a Non-canonical Vasopressin-Glutamate Pathway? *Front Neural Circuits*. 2016; **10**13.
655 4. Zhang L, Padilla-Flores T, Hernandez VS, Zetter MA, Campos-Lira E, Escobar LI,
656 Millar RP, Eiden LE. Vasopressin acts as a synapse organizer in limbic regions by boosting
657 PSD95 and GluA1 expression. *J Neuroendocrinol*. 2022e13164.
658 5. Zhang L, Medina MP, Hernandez VS, Estrada FS, Vega-Gonzalez A.
659 Vasopressinergic network abnormalities potentiate conditioned anxious state of rats
660 subjected to maternal hyperthyroidism. *Neuroscience*. 2010; **168**(2): 416-28.
661 6. Hernandez VS, Hernandez OR, Perez de la Mora M, Gomora MJ, Fuxe K, Eiden LE,
662 Zhang L. Hypothalamic Vasopressinergic Projections Innervate Central Amygdala
663 GABAergic Neurons: Implications for Anxiety and Stress Coping. *Front Neural Circuits*.
664 2016; **10**92.
665 7. Hernandez VS, Vazquez-Juarez E, Marquez MM, Jauregui-Huerta F, Barrio RA,
666 Zhang L. Extra-neurohypophyseal axonal projections from individual vasopressin-
667 containing magnocellular neurons in rat hypothalamus. *Front Neuroanat*. 2015; **9**130.
668 8. Campos-Lira E, Kelly L, Seifi M, Jackson T, Giesecke T, Mutig K, Koshimizu TA,
669 Hernandez VS, Zhang L, Swinny JD. Dynamic Modulation of Mouse Locus Coeruleus
670 Neurons by Vasopressin 1a and 1b Receptors. *Front Neurosci*. 2018; **12**919.
671 9. Hernandez-Perez OR, Crespo-Ramirez M, Cuza-Ferrer Y, Anias-Calderon J, Zhang
672 L, Roldan-Roldan G, Aguilar-Roblero R, Borroto-Escuela DO, Fuxe K, Perez de la Mora M.
673 Differential activation of arginine-vasopressin receptor subtypes in the amygdaloid
674 modulation of anxiety in the rat by arginine-vasopressin. *Psychopharmacology (Berl)*. 2018;
675 **235**(4): 1015-27.
676 10. DeVito LM, Konigsberg R, Lykken C, Sauvage M, Young WS, 3rd, Eichenbaum H.
677 Vasopressin 1b receptor knock-out impairs memory for temporal order. *J Neurosci*. 2009;
678 **29**(9): 2676-83.
679 11. Cilz NI, Cymerblit-Sabba A, Young WS. Oxytocin and vasopressin in the rodent
680 hippocampus. *Genes Brain Behav*. 2019; **18**(1): e12535.
681 12. Caldwell HK, Wersinger SR, Young WS, 3rd. The role of the vasopressin 1b receptor
682 in aggression and other social behaviours. *Progress in Brain Research*. 2008; **170**65-72.
683 13. Paul MJ, Peters NV, Holder MK, Kim AM, Whylings J, Terranova JI, de Vries GJ.
684 Atypical Social Development in Vasopressin-Deficient Brattleboro Rats. *eNeuro*. 2016; **3**(2).
685 14. Schatz KC, Kyne RF, Parmeter SL, Paul MJ. Investigation of social, affective, and
686 locomotor behavior of adolescent Brattleboro rats reveals a link between vasopressin's
687 actions on arousal and social behavior. *Horm Behav*. 2018; **106**1-9.
688 15. Frank E, Landgraf R. The vasopressin system--from antidiuresis to psychopathology.
689 *Eur J Pharmacol*. 2008; **583**(2-3): 226-42.
690 16. Young LJ. Oxytocin and vasopressin as candidate genes for psychiatric disorders:
691 lessons from animal models. *Am J Med Genet*. 2001; **105**(1): 53-4.

692 17. Inyushkin AN, Orlans HO, Dyball RE. Secretory cells of the supraoptic nucleus have
693 central as well as neurohypophysial projections. *J Anat*. 2009; **215**(4): 425-34.
694 18. Zhang L, Hernandez VS. Synaptic innervation to rat hippocampus by vasopressin-
695 immuno-positive fibres from the hypothalamic supraoptic and paraventricular nuclei.
696 *Neuroscience*. 2013; **228**139-62.
697 19. Santiago AC, Shammah-Lagnado SJ. Efferent connections of the nucleus of the
698 lateral olfactory tract in the rat. *J Comp Neurol*. 2004; **471**(3): 314-32.
699 20. McDonald AJ. Cytoarchitecture of the nucleus of the lateral olfactory tract: a Golgi
700 study in the rat. *Brain Res Bull*. 1983; **10**(4): 497-503.
701 21. Garcia-Lopez M, Abellan A, Legaz I, Rubenstein JL, Puelles L, Medina L.
702 Histogenetic compartments of the mouse centromedial and extended amygdala based on gene
703 expression patterns during development. *J Comp Neurol*. 2008; **506**(1): 46-74.
704 22. Moy SS, Nadler JJ, Perez A, Barbaro RP, Johns JM, Magnuson TR, Piven J, Crawley
705 JN. Sociability and preference for social novelty in five inbred strains: an approach to assess
706 autistic-like behavior in mice. *Genes Brain Behav*. 2004; **3**(5): 287-302.
707 23. Wee BE, Francis TJ, Lee CY, Lee JM, Dohanich GP. Mate preference and avoidance
708 in female rats following treatment with scopolamine. *Physiol Behav*. 1995; **58**(1): 97-100.
709 24. Dunn FL, Brennan TJ, Nelson AE, Robertson GL. The role of blood osmolality and
710 volume in regulating vasopressin secretion in the rat. *J Clin Invest*. 1973; **52**(12): 3212-9.
711 25. Paxinos G, and Watson, C. . *The Rat Brain in Stereotaxic Coordinates* Amsterdam.,
712 2006.
713 26. Perez de la Mora M, Lara-Garcia D, Jacobsen KX, Vazquez-Garcia M, Crespo-
714 Ramirez M, Flores-Gracia C, Escamilla-Marvan E, Fuxe K. Anxiolytic-like effects of the
715 selective metabotropic glutamate receptor 5 antagonist MPEP after its intra-amygdaloid
716 microinjection in three different non-conditioned rat models of anxiety. *Eur J Neurosci*.
717 2006; **23**(10): 2749-59.
718 27. Zhang L, Hernandez VS, Liu B, Medina MP, Nava-Kopp AT, Irles C, Morales M.
719 Hypothalamic vasopressin system regulation by maternal separation: its impact on anxiety in
720 rats. *Neuroscience*. 2012; **215**135-48.
721 28. Zhang L, Hernandez VS, Swinny JD, Verma AK, Giesecke T, Emery AC, Mutig K,
722 Garcia-Segura LM, Eiden LE. A GABAergic cell type in the lateral habenula links
723 hypothalamic homeostatic and midbrain motivation circuits with sex steroid signaling.
724 *Transl Psychiatry*. 2018; **8**(1): 50.
725 29. Mori K, Sakano H. Olfactory Circuitry and Behavioral Decisions. *Annu Rev Physiol*.
726 2021; **83**231-56.
727 30. Sugai T, Yamamoto R, Yoshimura H, Kato N. Multimodal cross-talk of olfactory and
728 gustatory information in the endopiriform nucleus in rats. *Chem Senses*. 2012; **37**(8): 681-8.
729 31. Seabrook TA, Burbridge TJ, Crair MC, Huberman AD. Architecture, Function, and
730 Assembly of the Mouse Visual System. *Annu Rev Neurosci*. 2017; **40**499-538.

731 32. Knipper M, Van Dijk P, Nunes I, Ruttiger L, Zimmermann U. Advances in the
732 neurobiology of hearing disorders: recent developments regarding the basis of tinnitus and
733 hyperacusis. *Prog Neurobiol*. 2013; **111**17-33.
734 33. Knierim JJ. The hippocampus. *Curr Biol*. 2015; **25**(23): R1116-21.
735 34. Vann SD, Aggleton JP, Maguire EA. What does the retrosplenial cortex do? *Nat Rev*
736 *Neurosci*. 2009; **10**(11): 792-802.
737 35. Matsuda T, Hiyama TY, Niimura F, Matsusaka T, Fukamizu A, Kobayashi K,
738 Kobayashi K, Noda M. Distinct neural mechanisms for the control of thirst and salt appetite
739 in the subfornical organ. *Nat Neurosci*. 2017; **20**(2): 230-41.
740 36. Zimmerman CA, Leib DE, Knight ZA. Neural circuits underlying thirst and fluid
741 homeostasis. *Nat Rev Neurosci*. 2017; **18**(8): 459-69.
742 37. Krettek JE, Price JL. A description of the amygdaloid complex in the rat and cat with
743 observations on intra-amygdaloid axonal connections. *J Comp Neurol*. 1978; **178**(2): 255-
744 80.
745 38. Zhang L, Hernandez VS, Gerfen CR, Jiang SZ, Zavala L, Barrio RA, Eiden LE.
746 Behavioral role of PACAP signaling reflects its selective distribution in glutamatergic and
747 GABAergic neuronal subpopulations. *Elife*. 2021; **10**.
748 39. Garcia-Calero E, Lopez-Gonzalez L, Martinez-de-la-Torre M, Fan CM, Puelles L.
749 Sim1-expressing cells illuminate the origin and course of migration of the nucleus of the
750 lateral olfactory tract in the mouse amygdala. *Brain Struct Funct*. 2021; **226**(2): 519-62.
751 40. Murakami G, Hunter RG, Fontaine C, Ribeiro A, Pfaff D. Relationships among
752 estrogen receptor, oxytocin and vasopressin gene expression and social interaction in male
753 mice. *Eur J Neurosci*. 2011; **34**(3): 469-77.
754 41. Flanagan LM, Pfaus JG, Pfaff DW, McEwen BS. Induction of FOS immunoreactivity
755 in oxytocin neurons after sexual activity in female rats. *Neuroendocrinology*. 1993; **58**(3):
756 352-8.
757 42. Cho MM, DeVries AC, Williams JR, Carter CS. The effects of oxytocin and
758 vasopressin on partner preferences in male and female prairie voles (Microtus ochrogaster).
759 *Behav Neurosci*. 1999; **113**(5): 1071-9.
760 43. Song Z, Larkin TE, Malley MO, Albers HE. Oxytocin (OT) and arginine-vasopressin
761 (AVP) act on OT receptors and not AVP V1a receptors to enhance social recognition in adult
762 Syrian hamsters (Mesocricetus auratus). *Horm Behav*. 2016; **81**20-7.
763 44. Gabor CS, Phan A, Clipperton-Allen AE, Kavaliers M, Choleris E. Interplay of
764 oxytocin, vasopressin, and sex hormones in the regulation of social recognition. *Behav*
765 *Neurosci*. 2012; **126**(1): 97-109.
766 45. Madlon-Kay S, Montague MJ, Brent LJN, Ellis S, Zhong B, Snyder-Mackler N,
767 Horvath JE, Skene JHP, Platt ML. Weak effects of common genetic variation in oxytocin
768 and vasopressin receptor genes on rhesus macaque social behavior. *Am J Primatol*. 2018;
769 **80**(10): e22873.
770 46. Wacker D, Ludwig M. The role of vasopressin in olfactory and visual processing.
771 *Cell Tissue Res*. 2019; **375**(1): 201-15.

47. Vaz RP, Cardoso A, Sá SI, Pereira PA, Madeira MD. The integrity of the nucleus of the lateral olfactory tract is essential for the normal functioning of the olfactory system. *Brain Struct Funct*. 2017; **222**(8): 3615-37.
48. Krause EG, de Kloet AD, Flak JN, Smeltzer MD, Solomon MB, Evanson NK, Woods SC, Sakai RR, Herman JP. Hydration state controls stress responsiveness and social behavior. *J Neurosci*. 2011; **31**(14): 5470-6.
49. de Bono M, Bargmann CI. Natural variation in a neuropeptide Y receptor homolog modifies social behavior and food response in C. elegans. *Cell*. 1998; **94**(5): 679-89.
50. Hernandez-Perez OR, Hernandez VS, Nava-Kopp AT, Barrio RA, Seifi M, Swinny JD, Eiden LE, Zhang L. A Synaptically Connected Hypothalamic Magnocellular Vasopressin-Locus Coeruleus Neuronal Circuit and Its Plasticity in Response to Emotional and Physiological Stress. *Front Neurosci*. 2019; **13**196.

Acknowledgments: We acknowledge support from DGAPA-UNAM (PAPIIT-IN216918, IG200121, LZ) and CONACYT (CB-238744) to LZ. MH002386, NIMH, NIH, USA (LEE). OH-P and MAZ were supported by Post-Doctoral Scholarship Program at UNAM (POSDOC-DGAPA).

Data availability: The data that support the findings of this study are available from the corresponding author upon reasonable request.

Supplementary information

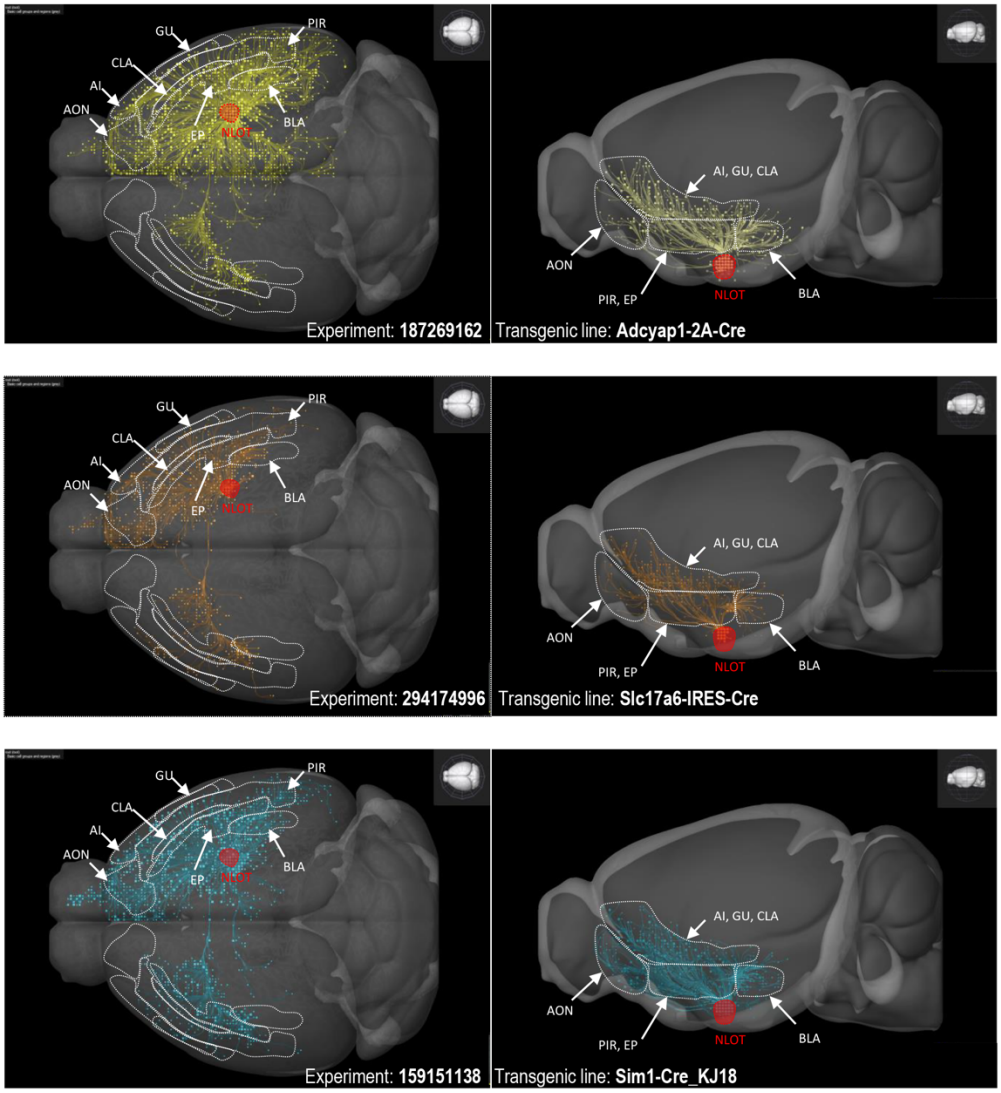

Nucleus of lateral olfactory tract (NLOT) neurons with different neurochemical markers share similar projection targets in cortical regions. Three dimensional projection patterns in dorso-ventral (left) and sagittal (right) views of NLOT virally transfected neurons in which reporter gene expression was restricted by selective CRE expression driven by the promoters of PACAP (Adcyap1 2A Cre) shown here in yellow , VGLUT2 (Slc17a6 IRES Cre) shown in orange or *single minded homolog 1* (Sim1 Cre_KJ18) depicted in blue. Notice that for all the experiments the cortical regions that were presented in bold letters in the table 1 (delineated by white dotted lines) received strong innervation by glutamatergic / PACAPergic axons originated in NLOT (delineated by red dotted lines). All of these target regions displayed increased Fos activity after 48WD+3CST. Reconstructions of the projection pathways were generated using the *Brain Explorer 2* program of the Allen Institute for Brain Science and the data of the experiments 187269162, 294174996 and 159151138 that can be found in the *Mouse Brain Connectivity Atlas.* Abbreviations: AON: anterior olfactory nucleus, AI: agranular insular cortex, BLA: basolateral amygdala, CLA: claustrum, GU: gustatory cortex, NLOT: nucleus of the lateral olfactory tract, PIR: piriform cortex.